INTERNATIONAL JOURNAL OF AGRICULTURE & BIOLOGY
ISSN Print: 1560–8530; ISSN Online: 1814–9596
18F–020/2018/20–5–1193–1200
DOI: 10.17957/IJAB/15.0662
http://www.fspublishers.org

Full Length Article

Biomass-Based Rapeseed (*Brassica napus*) Pod Morphological Model

Weixin Zhang, Hongxin Cao*, Wenyu Zhang, Yan Liu, Daokuo Ge, Chunhuan Feng, Weitao Chen, Chuwei Song, SijunGe, Qian Zhang and Qian Wan
Institute of Agricultural Information, Jiangsu Academy of Agricultural Sciences, Nanjing, China
*For correspondence: caohongxin@hotmail.com

Abstract

The rapeseed pod number is one of the major components for rapeseed yield. Pod morphology plays an important role in rapeseed plant development and function. In this paper, we studied the quantitative relationships between rapeseed pod architecture indices and the corresponding organ biomass, and presented a biomass-based model of pod geometric parameters of rapeseed (*Brassica napus* L.), designed to explain effects of cultivars and environmental conditions on rapeseed pods morphogenesis. Various model variables, such as pod length, pod diameter, pod angles, and corresponding organ biomass. The models were validated with the independent experiment data, and the results suggested that these variables in rapeseed were remarkably consistent in observation and simulation. The partitioning coefficient values of pod biomass (CPPB) had a significant level at $p<0.001$, and the *RMSE* values, and the d_a values were 0.077 g g^{-1}, and 0.015 g g^{-1} (n=62), respectively. In our descriptive models have a good mechanism and interpretation; the ratio of pod body length to pod biomass (RPLW); the ratio of the pod stalk tangent angle (RPSTW), and the ratio of the pod stalk and body angle (RPSBW) were analyzed initially, which are able to correlate the organ biomass with its morphogenesis. Thus, the growth model can be associated with the morphological model via the organ biomass, and the Functional Structural Rapeseed Models (FSRMs) have been expanded. © 2018 Friends Science Publishers

Keywords: Rapeseed (*Brassica napus*); Pod; Biomass; Morphological structure; Model

Introduction

Rapeseed (*Brassica napus* L.) is the world's essential oil crop with great potential in the future. How to cultivate an ideal plant type and how to improvement of the rapeseed yield and quality through rapeseed crop model has become a new research focus in agricultural field. With the rapid development of the different crop models, many researchers have employed the required temperature to simulate the growing process of rapeseed, such as EPIC-rape, CERES-Rape, BRASNAP-PH, APSIM-Canola (Kiniry *et al*., 1995; Habekotte, 1997; Gabrielle *et al*., 1998; Robertson *et al*., 1999). In recent years, the development of rapeseed's functional structural plant models (FSRMs) has become a new trend in the study. Groer *et al*. (2007), Müller *et al*. (2007) combined the LEAFC3-N with FSPMs, established a model, which could respond to the environmental changes. To identify the relationship between the rapeseed geometric indices and the corresponding organ biomass, the development of the rapeseed leaf morphological structural models based on biomass were conducted (Cao *et al*., 2013; Zhang, 2013; Zhang *et al*., 2014, 2015).

The crop organ morphological model is one of the key technologies for visualization. By applying the system analysis principle and mathematical modeling technique, the morphogenesis model for the wheat spike and rice panicle was developed, attaining the visualization of the crop organs (Chen *et al*., 2007a; Wu *et al*., 2009; Ding *et al*., 2010; Liu, 2010; Lei *et al*., 2011). However, only a few available studies could be found regarding the rapeseed pod simulation model and visualization in the country and overseas. Liu and Jin (2003), Tang *et al*. (2007) established the dynamic relationship between the pod and physiological development time (PDT) for the accurate simulation of the rapeseed green area index. Yue *et al*. (2011) created the pod 3D morphological model based on the OpenGL platform, laying a technology foundation for constructing the rapeseed growth visualization, but the model is only a statistical model, and cannot respond to the environmental variations. The FSPMs, also known as virtual crops, can accurately reproduce the crop organs' morphology. However, it was only involved in the vegetative growth stage in the previous study (Zhang, 2013), and the rapeseed pod morphology model based on the biomass has not yet been reported.

The number of pods, seeds per pod, and the seed weight determines the rapeseed yield per plant. Some researchers noted that the pod area of rapeseed increased and the leaf area index decreased during the post-flowering (Diepenbrock, 2000; Wang *et al*., 2014, 2016), and the

To cite this paper: Zhang, W., H. Cao, W. Zhang, Y. Liu, D. Ge, C. Feng, W. Chen, C. Song, S. Ge, Q. Zhang and Q. Wan, 2018. Biomass-based rapeseed (*Brassica napus*) pod morphological model. *Int. J. Agric. Biol*., 20: 1193–1200

green pod became the main organ on interception, absorption, and utilization of the effective energy. Song *et al*. (2010) reported that the spatial distribution of the pods may have an effect on the photosynthetic efficiency. In addition, it is one of the principle factors in determining the rapeseed plant yield.

The green pod is an essential organ of photosynthesis during the rapeseed maturity stage (Wang *et al*., 2014). It is both a sink and a source (Li *et al*., 1988; Song *et al*., 2010), which influences directly the photosynthetic capacity and final yield. Therefore, it is necessary to study the pod morphology that affected by the cultivars and environmental factors, and it is an indispensable part of the rapeseed plant morphological model. This paper explored the influence of the cultivars and environment conditions on the rapeseed pod morphology in a field experiment, linking the pod architecture parameters of rapeseed with biomass, by analyzing the field experimental data from 2011 to 2015, and developing the rapeseed pod morphological structural model, which is an important complement to the rapeseed morphological structural model, and the plant phenotypic group for rapeseed.

Materials and Methods

Experimental Details and Treatments

Experimental materials: Based on different primary ramification angles, the cultivars with three plant types, Ningyou 18, Ningyou 16, and Ningza 19, were selected, belonging to the *Brassica napus* species (Table 1).

Treatments: The field experiments were carried out at the site of Jiangsu Academy of Agricultural Sciences, Nanjing, China (32.03°N, 118.87°E) from 2011 to 2015 during the rapeseed-growing period. The soil type was the yellow-brown, and its basic nutrient statuses: organic carbon, 13.8 g kg^{-1}, nitrogen, 58.95 mg kg^{-1}, phosphorus, 29.25 mg kg^{-1}, potassium, 109.05 mg kg^{-1}, and pH 7.84. Three experiments were designed to implement (Table 2).

At the start of the pod growing stage, the five largest pods per plant were selected from the main anthotaxy axis and the primary ramification (PR) anthotaxy axis, respectively. The length of the pod body and pod stalk length, including the pod maximum diameter and pod angles, were measured. The pods were separated from the anthotaxy axis and in the paper bags, and placed in an oven with a temperature of the green of 105°C for 30 min, letting it stay in 80°C until they reached a stable weight.

The pod length was measured by the straight length of the pod beak from the top to the base. The pod maximum diameter was measured by the maximum length of the pod diameter value (at the base of the pod), and the average value was taken in multiple measurements. The pod stalk length was measured by the straight length of the pod body base to the point at the anthotaxy axis. Wang *et al*. (2015) reported that pod angle measurement results were not significantly between image analysis and protractor measurement methods. The pod stalk tangent angle was measured by the angle between the pod stalk and anthotaxy axis by protractor, and the average value was acquired by multiple measurements. The pod stalk and body angle were measured by the angle between the pod stalk and body by protractor, and average value was acquired by the multiple measurements (Fig. 1).

The angles of the pods play an essential role in the rapeseed yield and resistance and density tolerance. These determine directly the spatial distribution of the pod (Chen *et al*., 2007b; Shui *et al*., 2011). To accurately measure the pod angle, two new concepts were defined: the pod stalk tangent angle (PSTA) and the angle between pod stalk and pod body (PSBA). Both have a biological significance and enhanced mechanism in this study. The pod angle models can be expressed as follows:

$$\text{PSTA}(i) = \text{DWP}(i) \times \text{RPSTW}(i) \quad (1)$$

$$\text{PSBA}(i) = \text{DWP}(i) \times \text{RPSBW}(i) \quad (2)$$

Data Analysis

The MS Excel 2016 and SPSS version 19.0 were used to analyze the experimental data. Part of the data of the different cultivars and fertilizer levels was used for the modeling and parameter determination from 2012 to 2013. The remaining four-year independent data were employed for the model testing and inspection.

Model Validation

The root-mean-square-error (*RMSE*), correlation (*r*), mean absolute difference (d_a), ratio of d_a to the mean observation (d_{ap}), and 1:1 chart of the measured values and simulated values properties were used to validate the developed models in this paper (Cao *et al*., 2012). The smaller *RMSE*, d_a, and d_{ap} values, the better the consistency of simulated and observed values. The simulation results of the model will be proven accurate and reliable. The *RMSE*, d_a, and d_{ap} can be defined as:

$$RMSE = \sqrt{\frac{\sum_{i=1}^{n}(O_i - S_i)^2}{n}}$$

$$d_i = X_{Oi} - X_{Si}$$

$$d_a = \frac{\sum_{i=1}^{n} d_i}{n}$$

$$\overline{X}_O = \frac{\sum_{i=1}^{n} X_{Oi}}{n}$$

$$d_{ap} = \frac{|d_a|}{\overline{X}_O} \times 100\%$$

Where, i =sample number, X_{oi}=observed values, X_{si}=simulated values, n=total number of measurements.

Table 1: Experiment material and types of rapeseed

Name	Cultivar	Canopy morphology structure traits
Ningyou (V1)	18 Conventional	Half-vertical, the average plant height is 156.53cm, higher rank of the branch, the average angle of branching is 33.12°, the first effective branch number is 7.2, the effective pod number per plant is 361.6.
Ningyou (V2)	16 Conventional	Half-vertical, the average plant height is 157.50cm, the average angle of branching is 39.85°, the first effective branch number is 7.7, the effective pod number per plant is 347.49.
Ningza (V3)	19 Hybrid	Half-vertical, the average plant height is 163.10cm, the average angle of branching is 36.75°, the first effective branch number is 8.5, the effective pod number per plant is 420.

Table 2: Experimental designs

No.	Exp. time	Location	Cultivar	treatment
1	2011-2012	Farm of Jiangsu Academy of Agricultural Sciences,	V1, V3	N0, N2
2	2012-2015	Nanjing, China (32.03° N, 118.87° E)	V1, V2, V3	N1 D2
3	2012-2013		V1	N0, N1, N2 D1, D2, D3
4	2013-2015		V1, V3	N0, N1, N2, N3, N4 D2

N0, N1, N2, N3, and N4 represent the different fertilization levels; D1, D2, and D3 are the different density levels

Results

Pod Body Length Model

The experimental data showed that the pod body length on the main anthotaxy axis and the PR anthotaxy axis with the pod biomass is increasing trend (Fig. 2). The pod body length models can be expressed as follows:

$$PBL(i)=CPPB(i)\times(DW_{CP}(i)/DES\pm SDW_{SP}(i))\times RPLW(i) \quad (3)$$

Where, PBL(i) is the maximum pod body length on the ith d after emergence (cm). RPLW(i) is the ratio of the pod body length to the pod biomass (cm g^{-1}). CPPB(i) is the ratio of the pod biomass to the single aboveground part (g g^{-1}) on the ith d after emergence. $SDW_{SP}(i)$ was the standard error of biomass per plant on the ith d after emergence (determined by experiment) (g $plant^{-1}$). $DW_{CP}(i)$ was the biomass in canopy per area on the ith d after emergence (g m^{-1}). And, DES was the plant number per area (plant m^{-1}) (as a parameter of cultivation practices).

In Fig. 3 we have presented the relationship between the ratio of corresponding growth days to the whole growth period days of rapeseed (TI) and the ratio of the pod body length to the pod biomass (RPLW(i)) for main anthotaxy axis and PR anthotaxy axis. The data from 2012 to 2013 experiment showed that the values of RPLW(i) of different treatments with TI were close to S curve (Eq. 4) with significant r=0.940 (n=75, $r_{(73,0.001)}$=0.373, p<0.001) and R^2=0.883, and r=0.894 (n=395, $r_{(393,0.001)}$=0.165, p<0.001) and R^2=0.800, respectively (Fig. 3). The a_1, b_1, a_2, and b_2 are the model parameters whose values and testing results shown in Table 3.

$$RPLW(i)=\begin{cases} e^{a_1+b_1/TI} & \text{on the main anthotaxy axis} \\ e^{a_2+b_2/TI} & \text{on the PR anthotaxy axis} \end{cases} \quad \text{……...(4)}$$

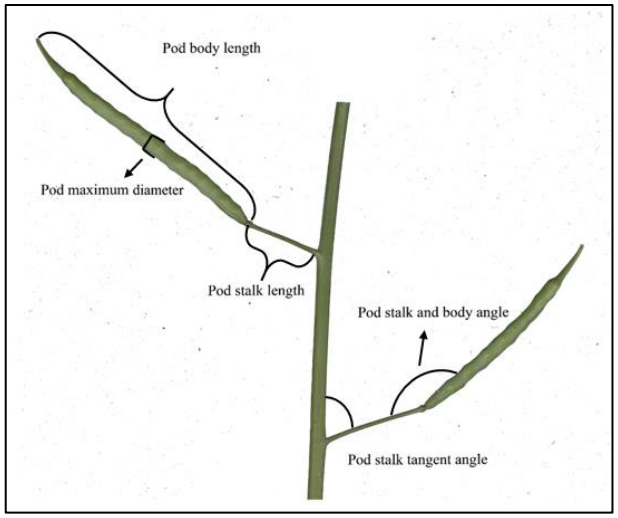

Fig. 1: Pod schematic diagram and measurement

The data from 2012 to 2013 experiment showed that the variation of the ratio of the pod biomass to the whole single aboveground plant (CPPB(i)) with TI can be described by an S curve model (Eq. 5) and the significant r=0.876 (n=76, $r_{(74,0.001)}$=0.370, p<0.001) and R^2=0.767 (Fig. 4). The A and B are the model parameters whose values and testing results shown in Table 3.

$$CPPB(i)=e^{A+B/TI} \quad \text{…….(5)}$$

Pod Stalk Length Model

According to the data from 2012 to 2013 experiment, the values of the pod stalk length (PSL(i)) of different treatments with the pod body length (PBL(i)) on the main anthotaxy axis and PR anthotaxy axis were close to quadratic function. Also we can see that the data points in Fig. 5B are more scattered than the data in Fig. 5A.

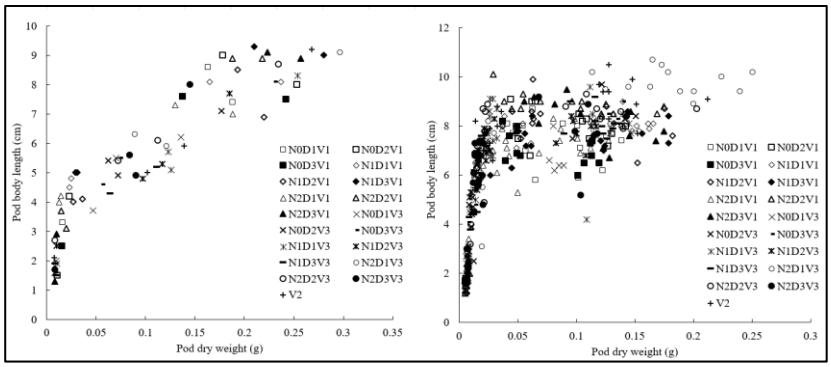

A. the main anthotaxy axis B. the PR anthotaxy axis

Fig. 2: The variation of the pod body length with the pod biomass from 2012 to 2013

N0D1V1: V1 with no fertilizer and low density. N0D2V1: V1 with no fertilizer and medium density, N0D3V1: V1 with no fertilizer and high density, N1D1V1: V1 with normal fertilizer and low density, N1D2V1: V1 with normal fertilizer and medium density, N1D3V1: V1 with normal fertilizer and high density, N2D1V1: V1 with high fertilizer and low density, N2D2V1: V1 with high fertilizer and medium density, N2D3V1: V1 with high fertilizer and high density. V2 and V3 with the same meaning as V1

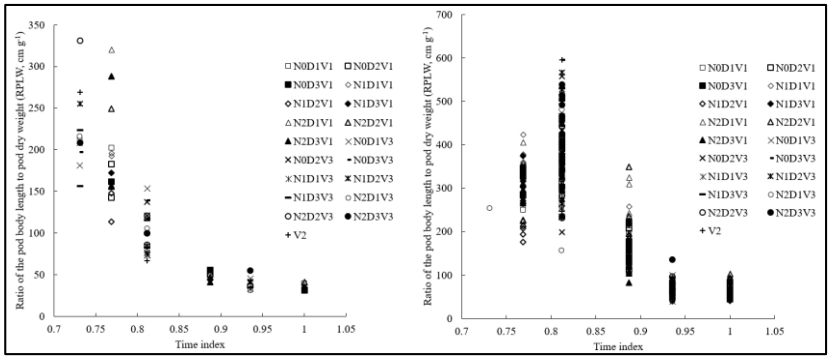

A. the main anthotaxy axis B. the PR anthotaxy axis

Fig. 3: The variation of the RPLW with the TI from 2012 to 2013

The significant r=0.257 (n=75, $r_{(73,\ 0.05)}$ =0.227, p<0.05) and R^2=0.066, and r=0.107 (n=395, $r_{(393,0.05)}$=0.098, p<0.05) and R^2=0.012, respectively (Fig. 5).Obviously, both of the coefficients of determination were low. The parameter coefficient c_1 and c_2 of eq. 6 were significant at p<0.001 (Table 3).

$$\mathrm{PSL(i)} = \begin{cases} a_3 PBL^2 + b_3 PBL + c_1 & \text{on the main anthotaxy axis} \\ a_4 PBL^2 + b_4 PBL + c_1 & \text{on the PR anthotaxy axis} \end{cases} \quad \text{.....(6)}$$

Pod Maximum Diameter Model

According to the data from 2012 to 2013 experiment, the pod maximum diameter PMD (*i*), of different cultivars changed with the pod body length on main anthotaxy axis and PR anthotaxy axis could be expressed as the power function (Eq. 7) with significant r=0.914 (n=75, $r_{(73,\ 0.001)}$ =0.373, p<0.001) and R^2=0.835, and r=0.928 (n=395, $r_{(393,\ 0.001)}$ =0.165, p<0.001) and R^2=0.862, respectively (Fig. 6). The a_5, b_5, a_6, and b_6 are model parameters whose values and testing results shown in Table 3.

$$\mathrm{PMD(i)} = \begin{cases} a_5 PBL^{b_5} & \text{on the main anthotaxy axis} \\ a_6 PBL^{b_6} & \text{on the PR anthotaxy axis} \end{cases} \quad \text{.....(7)}$$

Pod Angles Model

Ratio of pod stalk tangent angle: The experimental data showed that the ratio of pod stalk tangent angle, RPSTW (*i*), of different cultivars changed with the TI on main anthotaxy axis and PR anthotaxy axis could be expressed as the power function (Eq. 8) with significant r=0.914 (n=33, $r_{(31,\ 0.001)}$ =0.546, p<0.001) and R^2=0.835, and r=0.861 (n=248, $r_{(246,\ 0.001)}$ =0.208, p<0.001) and R^2=0.741, respectively (Fig. 7). The a_7, b_7, a_8, and b_8 are model parameters whose values and testing results shown in Table 3.

$$\mathrm{RPSTW(i)} = \begin{cases} a_7 TI^{b_7} & \text{on the main anthotaxy axis} \\ a_8 TI^{b_8} & \text{on the PR anthotaxy axis} \end{cases} \quad (8)$$

Table 3: The determination of model parameters and significance test

Architectural parameter	*Eq.*	*n*	Parameter Symbolic	Unstandardized Coefficients	*F*	*t*
RPLW	$e^{a_1+b_1/TI}$	75	a_1	-2.401	552.038***	-8.123***
			b_1	5.735		23.495***
	$e^{a_2+b_2/TI}$	395	a_2	-2.961	1572.921***	-14.505***
			b_2	7.000		39.660***
CPPB	$e^{A+B/TI}$	76	A	9.022	243.494***	10.882***
			B	-10.678		-15.604***
PSL	$a_3PBL^2+b_3PBL+c_1$	75	a_3	0.020	2.536	2.199
			b_3	-0.233		-2.248
			c_1	3.881		16.525***
	$a_4PBL^2+b_4PBL+c_2$	395	a_4	0.009	2.282	2.135
			b_4	-0.102		-2.077
			c_2	3.082		24.087***
PMD	a_5PBL^{b5}	75	a_5	0.061	369.413***	11.258***
			b_5	1.020		19.220***
	a_6PBL^{b5}	395	a_6	0.058	1459.806***	20.267***
			b_6	1.017		38.207***
RPSTW	a_7TI^{b7}	33	a_7	342.295	152.848***	8.654***
			b_7	-7.809		-12.363***
	a_8TI^{b8}	248	a_8	326.674	702.530***	12.459***
			b_8	-13.223		-26.505***
RPSBW	$a_9 TI^{b9}$	45	a_9	981.188	136.316***	11.732***
			b_9	-6.303		-11.675***
	$a_{10} TI^{b10}$	137	a_{10}	738.729	131.914***	7.845***
			b_{10}	-11.691		-11.485***

***, **, and * means p<0.001, p<0.01, and p<0.05, respectively. The same as below

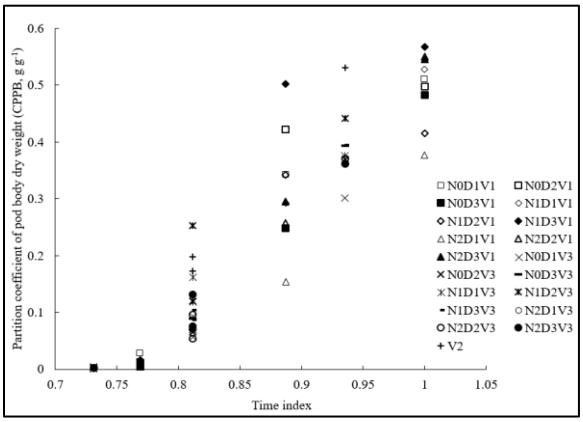

Fig. 4: The variation of the CPPB with the TI from 2012 to 2013

Ratio of pod stalk and pod body angle: The experimental data showed that the ratio of pod stalk tangent angle RPSBW(*i*), of different cultivars changed with the TI on main anthotaxy axis and PR anthotaxy axis could be expressed as the power function (Eq. 9) with significant r=0.872 (n=45, $r_{(43,\ 0.001)}$=0.474, p<0.001) and R^2=0.835, and r=0.703 (n=137, $r_{(135,\ 0.001)}$=0.278, p<0.001) and R^2=0.494, respectively. (Fig. 8). The a_9, b_9, a_{10}, and b_{10} are model parameters whose values and testing results all shown in Table 3.

$$\mathrm{RPSBW(i)} = \begin{cases} a_9 TI^{b_9} & \text{on the main anthotaxy axis} \\ a_{10} TI^{b_{10}} & \text{on the PR anthotaxy axis} \end{cases} \quad \ldots\ldots\ldots\ldots (9)$$

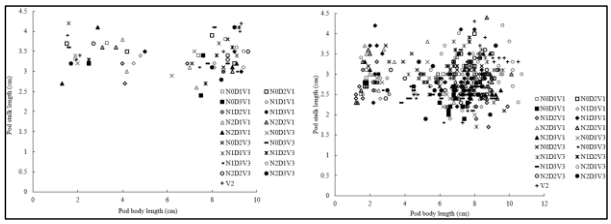

A. the main anthotaxy axis B. the PR anthotaxy axis

Fig. 5: The variation of the pod stalk length with the pod body length from 2012 to 2013

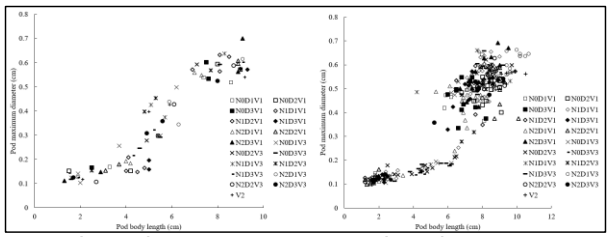

A. the main anthotaxy axis B. the PR anthotaxy axis

Fig. 6: The variation of the pod maximum diameter with the pod body length from 2012 to 2013

Model Validation

The biomass-based rapeseed pod morphological structural model proposed in this study were verified using the independent experimental data in 2011 to 2015, and the results showed that the correlation (r) of simulation and observation values all had significant level at p<0.001 exclude pod angles, and the average absolute difference (d_a), and the root mean square error (*RMSE*) were all smaller, the

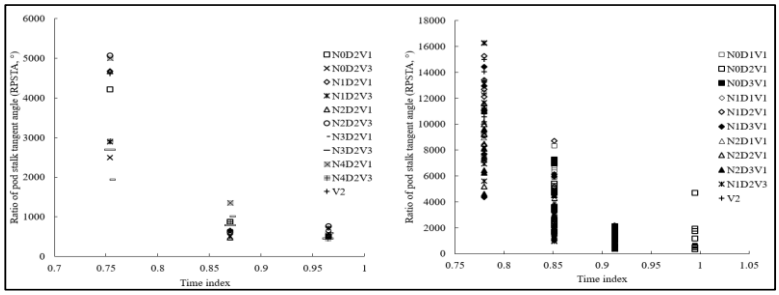

A. the main anthotaxy axis B. the PR anthotaxy axis

Fig. 7: The variation of the pod stalk tangent angle with the TI from 2012 to 2013

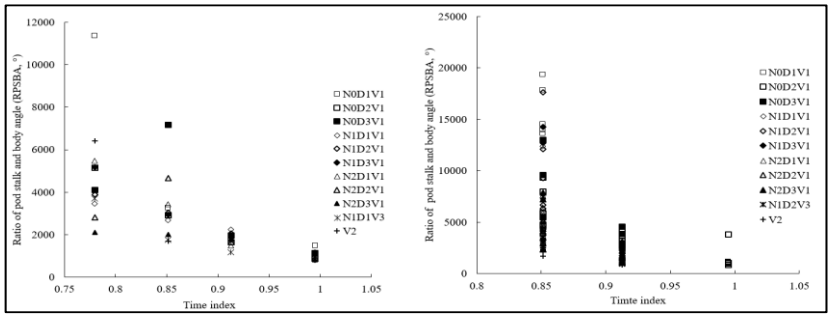

A. the main anthotaxy axis B. the PR anthotaxy axis

Fig. 8: The variation of the pod stalk and body angle with the TI from 2012 to 2013

ratio of d_a to the average observation (d_{ap}) were less than 5% for the pod stalk length and pod angles (Table 4) and the 1:1 line are represented in Fig. 9.

The correlation (r) of simulation and observation in rapeseed CPPB values were significant (p<0.001). Root mean square error (*RMSE*), and the average absolute difference (d_a) were all small. But the ratio of d_a to the average observation (d_{ap}) values was 6.67% which indicated that the model's accuracy was high (Table 4). The 1:1 line on simulation and observation in CPPB is represented in Fig. 9.

Discussion

Previous studies on pod physiology have reported that the rapeseed pod was affected by several environmental factors such as light intensity, temperature, and CO_2 (Rood *et al*., 1984; Habekotte, 1997; Poorter and Nagel, 2000; Baux *et al*., 2008; Vuorinen *et al*., 2014). The biomass allocation to the different plant organs depends on the cultivars and the ambient environment (Poorter and Nagel, 2000). In this paper, the effects of cultivars and environmental conditions were noted on rapeseed pods morphogenesis, with emphasis on the biomass as the main lines, presenting the biomass-based rapeseed pods' morphological structural model through the morphological observation and systematic analysis of the pods for many years.

As seen, from the dry matter production models, DW_{CP} (i) values were derived from the rapeseed photosynthesis and dry matter production and leaf area index models (Cao *et al*., 2006). We can estimate the responses to the cultivars and environment factors on DW_{CP} (i) values by the models. The pod length models proposed in this study connected the rapeseed growth model via organ biomass. The plant growth models can achieve the combination of the structures with their functions, relate the effects of environmental factors on the rapeseed aboveground morphogenesis, and contribute to the development of the rapeseed FSPMs.

Here we have established among the CPPB (i), the ratio of the pod biomass to the whole single aboveground plant on the ith d after emergence and TI, the ratio of the corresponding growth days to the whole rapeseed growth period. The model could be described by an *S*-curve function, and the validation results showed that the model fitting was good.

As regards PSL and PMD models, the PBL was selected for an independent variable, which could help the rapeseed geometrical parameter models more simplified and flexible. The PSL models were represented by the quadratic function and the PMD models could be described by a power function.

The 1:1 plotting of simulated and observed values of the rapeseed pod morphological indices showed that the precision of PBL, PSL, and PMD models was not very good when d_{ap}>5% and the *RMSE* and d_a values were too high, but the significant level was at p<0.001.

The pod area is a key component in identifying the photosynthetic capacity in the rapeseed's late growth stage, while the pod body length and diameter are essential indicators of the pod area (Tang *et al*., 2008). Some researchers have shown that the pod body length attained the

Table 4: Comparison of statistical parameters of observation and simulation in rapeseed pod architectural parameter models in 2011–2015

Architectural parameter	*n*	d_a	d_{ap}(%)	*RMSE*	*r*	*Sig.*
Pod body length (cm)	509	-1.117	19.258	2.171	0.796^{***}	$r_{(500,0.001)}$=0.146
Pod maximum diameter (cm)	509	-0.042	13.860	0.121	0.733^{***}	$r_{(500,0.001)}$=0.146
Pod stalk length (cm)	509	-0.100	3.496	0.437	0.228^{***}	$r_{(500,0.001)}$=0.146
Pod stalk tangent angle (°)	95	-0.364	0.506	18.167	0.301^{**}	$r_{(93,0.01)}$=0.263
Pod stalk and body angle (°)	61	5.4	3.586	18.539	0.384^{**}	$r_{(59,0.01)}$=0.327
CPPB (g g^{-1})	62	0.015	6.667	0.077	0.944^{***}	$r_{(60,0.001)}$=0.408

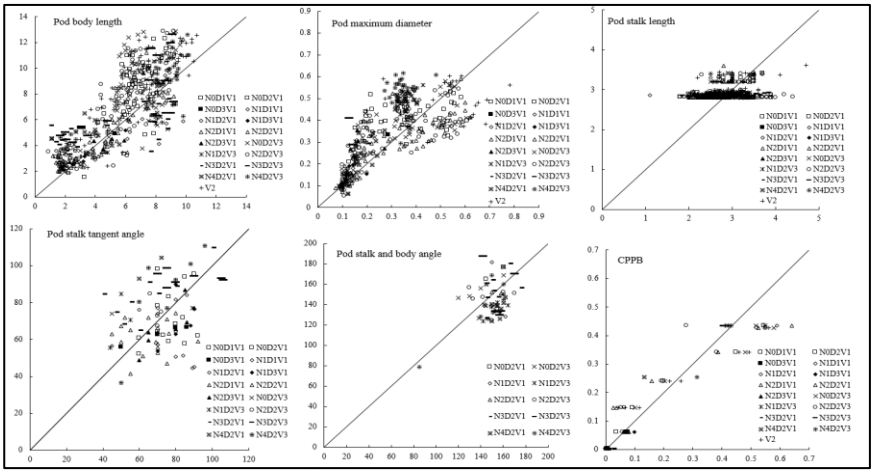

Fig. 9: Comparison of the observed with the simulated from 2011 to 2015

greatest value on its 15th day of post-flowering, and the diameter had a big change on 20th day (Pu *et al*., 1993; Li *et al*., 2011). In this paper, the relationship between the pod maximum diameter and pod body length (Fig. 6) showed that the pod body length and pod diameter from another point of view.

The pod stalk is the final tie of the rapeseed plant nutrition to the pod body, but some researchers considered the role of pod stalk on the rapeseed photosynthesis and final yield. Li *et al*. (2011) noted that the photosynthetic area of pod stalk is almost unaffected by the pod length and area. It is not the most critical organ relative to the pod body length and diameter, and the proportion of the pod stalk area to the total pod photosynthetic area is not that much. But in fact, the pod stalk plays a key role in the coupling of vegetative organs and reproductive organs (Leng *et al*., 2005). In our study, the relationship between the pod stalk length and the body length indicated that the variation ranges of the pod stalk length with the pod body length were between 2 and 4.5 cm, and the data points were somewhat scattered (Fig. 5B). The findings showed that the pod stalk length has a little effect on the pod body length, and the results also illustrated that the pod stalk length was influenced by the cultivars and environmental conditions.

Currently, there is little research on the pod angles. Zeng *et al*. (2014) claimed that the pod angles determined the spatial distribution of the pod, affecting the light-receiving and dry matter synthesis of rapeseed population from the past-flowering to its maturity. In this paper, the pod angles model could be described by a power function, and d_{ap}<5% and the *RMSE* and d_a values were small with the significant level of p<0.01.

Conclusion

In evaluating the relationships between the rapeseed pod architecture indices and the corresponding organ biomass, and developing the FSRMs, a biomass-based rapeseed pod morphological structural model was presented. Such models were designed to identify the effects of the cultivars and environmental factors on the rapeseed pod formation. The model validation with an independent experimental data indicated a good fitness between the simulated and observed values. The ratio of the pod body length to pod biomass (RPLW), the ratio of the pod stalk tangent angle to pod biomass (RPSTW), and the ratio of the pod stalk and body angel to pod biomass (RPSBW) of rapeseed were of great biological significance. The rapeseed pod morphological structural model in this paper is feasible, and may provide a reference for the rapeseed plant type in future breeding programs.

Acknowledgements

This work was supported by National Natural Science Foundation of China (31601223; 31471415; 31171455; 31201127), National High-Tech Research and Development

Program of China (2013AA102305-1), Jiangsu Province Agricultural Scientific Technology Innovation Fund [CX(14)2114], Jiangsu Academy of Agricultural Sciences Basic Scientific Research Work Special Fund [ZX(15)3003], and the Fund of Jiangsu Academy of Agricultural Sciences (No. 6111648).

References

Baux, A., T. Hebeisen and D. Pellet, 2008. Effects of minimal temperatures on low-linolenic rapeseed oil fatty-acid composition. *Eur. J. Agron*., 29: 102–107

Cao, H.X., J.S. Hanan, Y. Liu, Y.X. Liu, Y.B. Yue, D.W. Zhu, J.F. Lu, J.Y. Sun, C.L. Shi, D.K. Ge, X.F. Wei, A.Q. Yao, P.P. Tian and T.L. Bao, 2012. Comparison of crop model validation methods. *J. Integr. Agric*., 11: 1274–1285

Cao, H.X., C.L. Zhang, G.M. Li and Z.Q. Jin, 2006. Researches of simulation models of rape (*Brassica napus* L.) growth and development. *Acta Agron. Sin.*, 32: 1530–1536

Cao, H.X., W.Y. Zhang, W.X. Zhang, Y. Liu, Y.X. Liu, J.S. Hanan, Y.L. Chen, Y.B. Yue, Z.Y. Zhang, D.K. Ge, K.Y. Fu, Y.R. Sha and C.H. Feng, 2013. Biomass-based rapeseed (*Brassica napus* L.) leaf geometric parameter model. *Proceedings of the 7th International Conference on Functional-Structural Plant Models*, Saariselkä, Finland

Chen, G.Q., Y. Zhu, H. Liu and W.X. Cao, 2007a. Morphogenesis model-based virtual growth system for organs and plant of wheat. *Trans. CSAE*, 23: 126–130

Chen, X.J., C.K. Qi, H.M. Pu, J.F. Zhang, J.Q. Gao and S.Z. Fu, 2007b. Evaluation of lodging resistance in rapeseed (*Brassica napus* L.) and relationship between plant architecture and lodging resistance. *Chin. J. Oil Crop Sci*., 29: 54–57

Diepenbrock, W., 2000. Yield analysis of winter oilseed rape (*Brassica napus* L.): a review. *Field Crop Res*., 67: 35–49

Ding, W.L., C. Liu, Y.P. Zhang, D.F. Zhu, Q.Y. Zhang and H. Gu, 2010. Visually modeling spatial shape of rice panicle based on calculation of bending deformation. *Chin. J. Rice Sci*., 24: 309–314

Gabrielle, B., P. Denoroy, G. Gosse, E. Justes and M.N. Andersen, 1998. Development and evaluation of a CERES-type model for winter oil seed rape. *Field Crops Res*., 57: 95–111

Groer, C., O. Kniemeyer, R. Hemmerling, W. Kurth, H. Becker and G.H. Buck-Sorlin, 2007. A dynamic 3D model of rape (*Brassica napus* L.) computing yield components under variable nitrogen fertilization regimes. *5th International Workshop on Functional-Structural Plant Models*. Prusinkiewicz, P., J.S. Hanan and B. Lane (eds.). Napier, New Zealand: *Hort Res*., 4.1–4.4

Habekotte, B., 1997. Evalation of seed yield determining factors of winter oilseed rape (*Brassica napus*L.) by means of crop growth modelling. *Field Crop Res.*, 54: 137–151

Kiniry, J.R., D.J. Major, R.C. Lzaurralde, J.R. Williams, P.W. Gassman, M. Morrison, R. Bergentine and R.P. Zentener, 1995. EPIC model parameters for cereal, oil seed and forage crop in the north Great Plain region. *Can. J. Plant Sci*., 75: 679–688

Lei, X.J., L. Tang, Y.H. Zhang, H.Y. Jiang, W.X. Cao and Y. Zhu, 2011. Geometric model and visualization of wheat spike. *Trans. CSAE*, 27: 179–184

Leng, S.H., Y. Tang, Q.L. Li, Q.S. Zuo and P. Yang, 2005. Studies on source and sink of rapeseed I. Regulation of pod size on source and sink in rapeseed after flowering. *Chin. J. Oil Crop Sci.*, 27: 37–40

Li, C., J.H. Chen and W.Y. Shang, 1988. Study on the processes of the development of pods and seeds in *Brassica napus* L. *Chin. J. Oil Crop Sci*., 33: 197–206

Li, F.Y., J.G. He and C.Y. Guan, 2011. Research progress on rapeseed leaf and pod photosynthesis. *Crops Res*., 25: 405–409

Liu, C., 2010. The visual modeling study of rice panicles and roots. *MS Thesis*, Zhejiang University, Zhejiang, China

Liu, H. and Z.Q. Jin, 2003. A phonological model to simulate rape development. *J. Appl. Meteorol. Sin*., 14: 634–640

Müller, J., H. Braune, P. Wernecke and W. Diepenbrock, 2007. Towards universality and modularity: a generic photosynthesis and transpiration module for functional structural plant models. *In*: *5th International Workshop on Functional-Structural Plant Models*. Prusinkiewicz, P., J.S. Hanan and B. Lane (eds.). Napier, New Zealand. *Hort Res.*, 13.1–13.4

Poorter, H. and O. Nagel, 2000. The role of biomass allocation in the growth response of plants to different levels of light, CO_2, nutrients and water: a quantitative review. *Aust. J. Plant Physiol*., 27: 595–607

Pu, H.M., C.K. Qi and S.Z. Fu, 1993. Growth characteristics and source-sink effect of rapeseed pod. *Jiangsu Agric. Sci*., 3: 22–25

Robertson, M.J., J.F. Holland, J.A. Kirkegaard and C.J. Smith, 1999. Simulation growth and development of canola in Australia. *Proceedings of the 10th International Rapeseed Congress*. Canberra, Australia

Rood, S.B., D.J. Major and W.A. Charnetski, 1984. Seasonal changes in $^{14}CO_2$ assimilation and ^{14}C translocation in oilseed rape. *Field Crops Res*., 8: 341–348

Shui, H.X., T.Z. Tang and Y.Z. Niu, 2011. Relationship between endogenous hormones and pod-length development in *Brassica napus* L. *Agric. Sci. Tech*., 12: 710–714

Song, X., F.L. Liu, P.Y. Zheng, X.K. Zhang, G.Y. Lu, G.P. Fu and Y. Cheng, 2010. Correlation analysis between agronomic traits and yield of rapeseed (*Brassica napus* L.) for high-density planting. *Sci. Agric. Sin*., 43: 1800–1806

Tang, L., Y. Zhu and W.X. Cao, 2007. A simulation model for dynamic green area index in winter rapeseed (*Brassica napus*). *J. Plant Ecol*., 31: 897–902

Tang, L., Y. Zhu, T.M. Liu and W.X. Cao, 2008. A Process-based model for simulating phenological development in rapeseed. *Sci. Agric. Sin*., 41: 2493–2498

Vuorinen, A.L., M. Kalpio, K.M. Linderborg, M. Kortesniemi, K. Lehto, J. Niemi, B. Yang and H.P. Kallio, 2014. Coordinate changes in gene expression and triacylglycerol composition in the developing seeds of oilseed rape (*Brassica napus*) and turnip rape (*Brassica rapa*). *Food Chem.*, 145: 664–673

Wang, C.L., J.B. Hai, J.H. Tian, J.L. Yang and X.G. Zhao, 2014. Influence of silique and leaf photosynthesis on yield and quality of seed of oilseed rape (*Brassica napus* L.) after flowering. *Acta Bot. Boreali–Occid. Sin*., 34: 1620–1626

Wang, C.L., J.B. Hai, J.L. Yang, J.H. Tian, W.J. Chen, T. Chen, H.B. Luo and H. Wang, 2016. Influence of leaf and silique photosynthesis on seeds yield and seeds oil quality of oilseed rape (*Brassica napus* L.). *Eur. J. Agron.*, 74: 112–118

Wang, W.X., Q. Hu, D.S. Mei, Y.C. Li, H. Wang, J. Wang, L. Fu and J. Liu, 2015. Evaluation of branch and pod angle measurement based on digital images from *Brassica napus* L. *Chin. J. Oil Crop Sci*., 37: 566–570

Wu, Y.L., L. Tang, X.J. Liu, W.Y. Zhang, W.X. Cao and Y. Zhu, 2009. Architectural parameter-based geometric modeling and visualization of rice panicle. *Sci. Agric. Sin*., 42: 1190–1196

Yue, Y.B., Y. Zhu and H.X. Cao, 2011. Models- and OpenGL-based visual technology for rapeseed (*Brassica napus* L.) pod. *Jiangsu Agric. Sci*., 438–441

Zeng, C., C.J. Liu, H.Z. Xu, Y. Huang and S.L. Yi, 2014. The research progress about plant type breeding of rape. *Chin. Agric. Sci. Bull*., 30: 14–18

Zhang, W.X., 2013. Study on biomass-based rapeseed (*Brassica napus* L.) aboveground morphological structure model. *MS Thesis*, Nanjing Agricultural University, Nanjing, China

Zhang, W.X., H.X. Cao, Y. Zhu, Y. Liu, W.Y. Zhang, Y.L. Chen and K.Y. Fu, 2015. Morphological structure model of leaf space based on biomass at pre-overwintering stage in rapeseed (*Brassica napus* L.) plant. *Acta Agron. Sin*., 41: 318–328

Zhang, W.Y., W.X. Zhang, D.K. Ge, H.X. Cao, Y. Liu, K.Y. Fu, C.H. Feng and W.T. Chen, 2014. A biomass-based leaf curve model for rapeseed (*Brassica napus* L.). *Jiangsu J. Agric. Sci*., 30: 1259–1266

(Received 29 January 2018; Accepted 28 February 2018)